Thermoelectric Energy Harvesting on Rotation Machines for Wireless Sensor Network in Industry 4.0

1st Adelson D. dos Santos
University of Campinas
Campinas, Brazil
adelson@dsif.fee.unicamp.br

2nd Silvio C. de Brito
Federal Institute of São Paulo
Campinas, Brazil
silvio.col@aluno.ifsp.edu.br

3rd Anderson V. Martins
University of Campinas
Campinas, Brazil
vedoveto@dsif.fee.unicamp.br

4th Filipe Figueredo Silva
TECHPLUS
Campinas, Brazil
filipe.ads@protonmail.com

5th Flávio Morais
Sao Paulo State University (UNESP)
Tupã, Brazil
flavio.morais@unesp.br

***Abstract*—We propose an autonomous energy wireless sensor node for monitoring rotation machines condition. The thermal energy dissipated during normal operation of the motor can be harvested to power an ultra low power wireless sensor. The harvested energy is stored in supercapacitors instead of lithium-ion battery, providing an extended life for the energy storage element and being able to handle high energy radio transmission pulses. The proposed system may be used on early fault diagnosis through pervasive data collection of machines condition. The collected data can provide a maintenance schedule programming with low impact in plant operation, reducing unexpected production stop due motors failures.**

***Index Terms*—autonomous energy wireless sensor, energy harvesting, supercapacitors, ultra-low-power, early fault diagnosis, preventive maintenance.**

I. Introduction

Wireless communication forms part of industries reality. Autonomous energy sensors distributed in a wide area sending real time monitoring of critical equipment can enable early fault diagnosis through pervasive data collection [1]. Additionally, these sensors are the key for growing customized demand and green production, and the foundation for realization of the Industry 4.0 [2].

Industry 4.0 is a term formulated at the Hannover Fair in 2011 that describes the creation of smart factories with virtual and physical manufacturing systems that globally cooperate with each other in a flexible way, enabling the creation of new operation models [3]. Therefore, industrial wireless sensor networks (IWSN) plays a important role in this context.

Usually, IWSN are battery-powered field devices far from energy sources and sometimes in places that are difficult to access, which increases efforts to replace them [4]. Energy harvesting techniques applies to this scenario in order to ensure a complementary or main energy source, increasing energy storage system life and creating an autonomous energy sensor node.

Rotating machines are widely used in industry and their unexpected breakdowns have major impact on plant operation, causing raw material and economic losses [5]. In order to reduce plant operation interruption, vibration monitoring is the most commonly applied method in motoring fault diagnosis in industries [5], [6]. Thus, the presence of autonomous energy IWSN for monitoring motor vibrations in industry sites can enable opportunities in terms of sensor energy efficiency and fault diagnosis for industrial systems.

This work proposes an autonomous energy sensor node for monitoring the health of motors based on the vibration method and using its dissipated heat as an energy source.

grant #2017/16053-7, Sao Paulo Research Foundation (FAPESP).

II. Energy autonomous sensor node description

The proposed sensor node can be separated in thermoelectric energy harvesting, power management circuits and sensor. This work firstly covers the thermoelectrical generator used to harvest thermal energy dissipated by motors. Next, it addresses voltage conditioning through power management circuits, and energy storage systems. Finally, it describes the sensor itself (sensor node) and its characteristics.

A. Thermoelectrical Generator

Thermoelectricity is a phenomenon that relates to heat and electricity. Thermoelectric generator (TEG) uses this behavior to provide electricity from temperature difference. They are constructed with a set of thermoelectric (TE) modules inserted between two heat exchangers, that convert a part of the thermal energy that flows through them into electricity [7].

For a TEG, the relation between produced electricity and gradient temperature is called the Seebeck coefficient (α), and it is an important parameter to observe when selecting a TEG for an application. Eq. (1) shows the relation between produced voltage (V_{TEG}) and temperature difference (ΔT) in relation to each side of TEG.

$$V_{TEG} = \alpha \Delta T \tag{1}$$

Internal resistance and produced voltage are important characteristics to observe when selecting a TEG, as resistance mismatches could reduce the available electrical power and may create a lack of output voltage to start-up power management circuits.

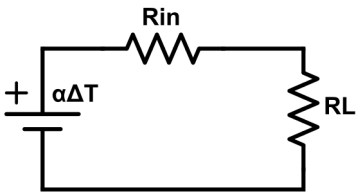

Fig. 1. TEG circuit model

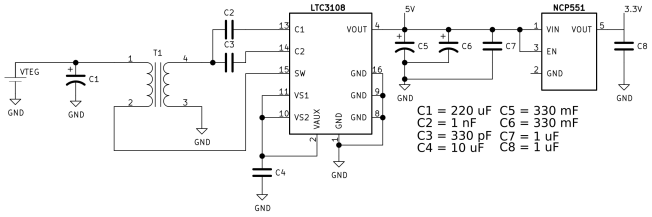

Fig. 2. Power management circuit

Applying Ohm's law in Fig.1, in which R_{in} is the TEG internal resistance and R_L is the load resistance, the TEG output power P_{TEG} can be described as:

$$P_{TEG} = \frac{\alpha \Delta T^2}{R_L + R_{in}} \cdot R_L \tag{2}$$

Notice that the maximum power transfer occurs when $R_L = R_{in}$.

In this paper, we used TEG241-1,0-1,2 from EVERREDtronics, in which specfications are shown in Table I for $\Delta T_{REF} = 110°C$:

TEG output power P_{TEG} for any temperature difference ΔT can be described as:

$$P_{TEG} = \frac{P_{REF}}{{\Delta T_{REF}}^2} \cdot \Delta T^2 \tag{3}$$

Applying Eq.(3) to the characteristics of the TEG described in Table I, we find the relation described in Eq.(4) of avaliable output power for any ΔT, in case of matched load.

$$P_{TEG} = 297,5 \mu W \cdot \Delta T^2 \tag{4}$$

Finally, the efficiency of TEG (η) can be described as ratio of TEG output power (P_{TEG}) generated from a passage of heat flow that passes through it (Q_{IN}), as presented in Eq.(5).

$$\eta(\%) = \frac{P_{TEG}}{Q_{IN}} \cdot 100 \tag{5}$$

Applying Eq.(5) for $P_{REF} = P_{TEG}$ and Q_{IN} from Table I, we find TEG efficiency $\eta_{TEG} = 5\%$.

B. Power management circuit

Although TEGs are highly reliable, their efficiency still stands at around 10% [7]. Additionally, produced voltage must be conditioned, as it must be stable and at acceptable levels to supply energy to the sensor.

The power management circuit is used to perform DC/DC conversion of input voltage and manage the charging a supercapacitor. The efficiency of this circuit must be as high as possible, since it is connected to a low efficency and extremely low voltage source. The power management circuit is presented in Fig.2. In order to perfom the power management we selected LTC3108 from Analog Devices. This integrated circuit has start-up voltage around at 50 mV when using 1:50 transformer that can provide 5 V in this output. The output value is stepped down to 3.3 V by low dropout linear regulator NCP551, in which has ultra low quiescent current of 4 μA. The presence of this regulator is necessary as it is responsible for stabilizing the 3.3 V sensor node, ensuring regulation even in abrupt voltage transient of supercapacitor in the 5 V to 3.3 V range.

A supercapacitor was used as energy storage system. It is suitable for this application because the autonomous sensors must transmit data wirelessly and radio transmissions are power hungry. A lithium-ion batteries are slow and can not able to handle fast charge and discharge cycles. Therefore, energy avaliable (E) can be described in terms of capacitance (C), initial voltage (V_1) and final voltage (V_2) as:

$$E = \frac{C \cdot (V_2 - V_1)^2}{2} \tag{6}$$

In terms of consumed power during sensor node on-state (P_{on}), we can rearrange Eq.(6) considering this period (T_{on}) and describe as:

$$P_{ON} = \frac{C \cdot (V_2 - V_1)^2}{2 \cdot T_{on}} \tag{7}$$

TABLE I
TEG SPECIFICATIONS

Dimensions (mm)	40x40
theoretical seedbeck coefficient (α_T)	110 mV/°C
open circuit voltage (V_{open})	12,1 V
matched load (R_{IN})	10 Ω
matched output power (P_{REF})	3.6 W

C. Sensor node

The sensor node comprises a low power, 3-axis analog accelerometer LIS 344ALH from STMicroelectronics and a Ultra-Low-Power Sub-1 GHz Wireless MCU CC1310 from Texas Instruments.

The accelerometer has selectable full-scale of ±2g/±6g and power-down mode that is set when no samples are acquired, contributing to the reduction in energy consumption. The voltage output of LIS 344ALH is sampled by Analog-to-digital converter embedded in MCU CC1310 at a sample frequency of 20 kHz, resulting in 800 samples in each axis that are transmitted wirelessly. Radio transmissions are made based on IEEE 802.15.4, using ISM 902-928 MHz bandwidth, that provides ultra-low power consumption, long range and low baudrate, characteristics that are well suited for our application. Finally, low-power programming routines were made in order to reach minimum energy consumption during the operation of sensor. Processor functions every 5 minutes to power up the accelerometer, measure and transmit data. The whole cycle is done in 1.370 s.

TABLE II
EXPERIMENTAL RESULTS OF THE TEG AND THE DC/DC CONVERTER INTERFACE

V_{OC}	343 mV
V_{INDCDC}	155.30 mV
η_{DCDC}	28%
P_{INDCDC}	3.19 mW
$P_{OUTDCDC}$	893 μW

III. EXPERIMENTAL RESULTS

Experimental tests were perfomed using the setup shown in Fig. 3.

A single-phase 350 W, 110 V induction motor, was used in order to check whether its dissipated heat can supply the system. We fixed a TEG on the motor fin and connected it to DC/DC converter. The output of the converter was connected to two parallel 330 mF EATON supercapacitor (KR-5R5V334-R) through breadboard, resulting in a 660 mF supercapacitor. The linear regulator and the accelerometer were assembled in same printed circuit board and they were connected between supercapacitors and CC3110, supplying energy to the sensor node. Finally, measured data are transmitted to a second node and connected to PC (Not shown in figure).

First, we measured the efficiency of DC/DC converter (η_{DCDC}) for input voltages in the 100 mV to 500 mV range. The results are shown in Fig.4. Efficiency values starts at 40% and decrease.

We evaluated the performance of the TEG and its interface with a DC/DC converter, as shown in 2. The measurements were done in room temperature (23 $^{\circ}C$) and the measured results are shown in Table II. The ratio of $V_{IN_{DCDC}}$ (input voltage of DC/DC converter) and V_{OC} is approximately 45%, showing that the impedance matching is almost perfect, therefore this interface operates near the maximum power transfer point. We measured $P_{OUT_{DCDC}}$ (DC/DC converter output power) and considered $\eta_{DCDC} \approx 28\%$ from Fig. 4, in order to calculate $P_{IN_{DCDC}}$ (DC/DC converter input power). Therefore, the sensor node must operate with power less than 1 mW.

The real temperature on each side of TEG could not be measured because our assembly does not provide access to it. However, an estimation of temperature difference can be

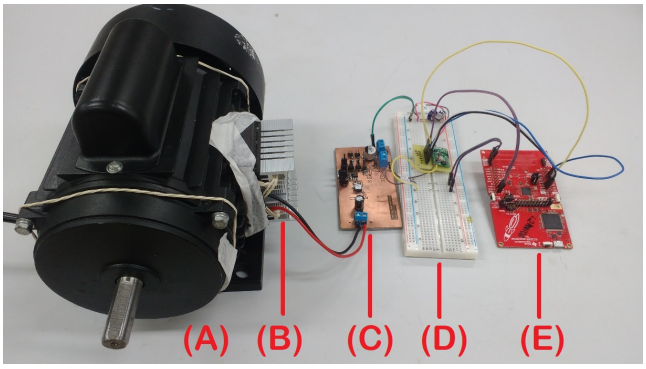

Fig. 3. Evaluated setup. (A) Induction motor. (B) TEG. (C) DC/DC converter. (D) Breadboard with supercapacitors, linear regulator and accelerometer. (E) MCU CC1310

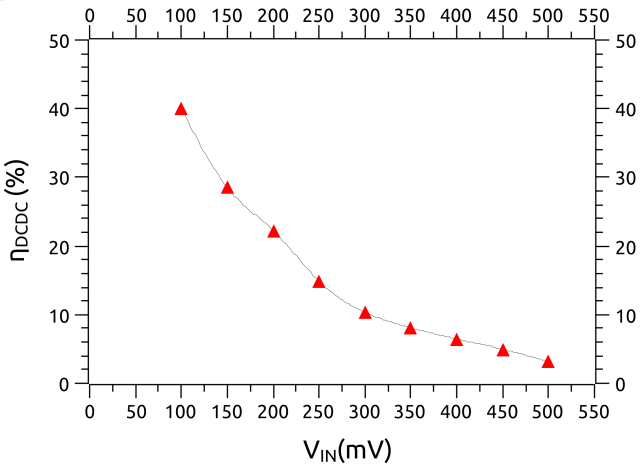

Fig. 4. Efficiency of DC/DC converter

TABLE III
THE TEG PARAMETERS RESULTS

Q_{IN}	68.3 mW
ΔT	3.27 $^{\circ}C$
α_{EXP}	104.75 mV/°C

done. Using Eq.(4) for measured $P_{TEG} = 3.19\,mW$ from Table II, the temperature difference between each side of TEG is $\Delta T = 3.27\,^{\circ}C$.

Addionally, the heat flow passing through TEG can be estimated employing Eq.(5) for $P_{TEG} = 3.19 mW$ and $\eta = 5\%$. The total heat flow going through TEG is $Q_{IN} = 63.8 mW$.

Finally, we calculated the seebeck coefficient of $\alpha_{EXP} = 104.75\ mV/^{\circ}C$ for this setup using Eq. (1) to measured $V_{OC} = 343\ mW$ and $\Delta T = 3.27\,^{\circ}C$. The results are summarized in Table III. The result of experimental seebeck coefficient has a deviation of 4.78% from the theoretical seebeck coefficient.

The sensor node was configured to do transmissions every 5 minutes. We acquire 800 samples per axis and, for minimizing voltage drop in the supercapacitor, 5 transmissions of 160 samples are done per axis. The energy for this transmissions come from the supercapacitor and the voltage waveform during the transmission of the three axis is presented in Fig.5.

Observing time and voltage variation of previous waveform we can calculate the average power (P_{AVG}).

Applying Eq.(7), for $T_{ON} = 900\ s$, $V_2 - V_1 = 860\ mV$ and $C = 660\,mF$ the average power consumption of sensor node working every 5 minutes is $P_{AVG} = 271\ \mu W$.

The minimum input voltage to maintain the linear regulator functioning properly is 3.34 V. Therefore, the maximum voltage variation on the supercapacitor is $V_2 - V_1 = 1.66\,V$. From Eq.(6) and $C = 660\,mF$, we estimated that the system has $E = 909,35\ mJ$ avaliable.

Finally, applying Eq.(6) for $V_2 - V_1 = 860\ mV$ and $C = 660\ mF$, we estimate that the system uses $E = 244,70\ mJ$ to measure and transmit. This value represents 26,9% of total energy avaliable and indicates that the sensor node could send other parameters, such as temperature, do retransmissions if needed or its period could be smaller than

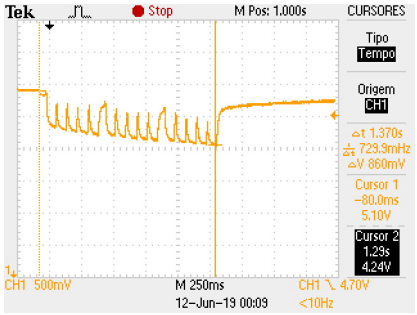

Fig. 5. Voltage waveform of supercapacitor during transmissions of 800 samples

5 minutes.

IV. Conclusions

We presented a proposal of an autonomous energy wireless sensor node powered by thermoelectric energy-harvesting generator that can be applied for a motor status monitoring based on vibration measurements.

We attached the TEG to the motor fin for capturing its dissipated heat. The energy harvested was 909.35 mJ from a temperature difference of 3.27 $^{\circ}C$. This available energy proved to be enough to maintain sensor node operating every 5 minutes, transmiting 800 samples per accelerometer axis, without any disturbance to the sensor node operation. Futhermore, consumption during transmissions were 244,70 mJ, representing 26,9% of total energy, indicating the cycle can be smaller than 5 minutes and retransmissions or transmissions of other parameters, such as temperature, is feasible.

Acknowledgment

This work was supported by FAPESP (2017/16053-7) and TECHPLUS through the PIPE program.

References

[1] F. Civerchia, S. Bocchino, C. Salvadori, E. Rossi, L. Maggiani, and M. Petracca, "Industrial internet of things monitoring solution for advanced predictive maintenance applications," *Journal of Industrial Information Integration*, vol. 7, pp. 4–12, 2017.

[2] X. Li, D. Li, J. Wan, A. V. Vasilakos, C.-F. Lai, and S. Wang, "A review of industrial wireless networks in the context of industry 4.0," *Wireless networks*, vol. 23, no. 1, pp. 23–41, 2017.

[3] K. Schwab, *The fourth industrial revolution*. Currency, 2017.

[4] S. Sudevalayam and P. Kulkarni, "Energy harvesting sensor nodes: Survey and implications," *IEEE Communications Surveys & Tutorials*, vol. 13, no. 3, pp. 443–461, 2010.

[5] L. Hou and N. W. Bergmann, "Novel industrial wireless sensor networks for machine condition monitoring and fault diagnosis," *IEEE transactions on instrumentation and measurement*, vol. 61, no. 10, pp. 2787–2798, 2012.

[6] Y. Wei, Y. Li, M. Xu, and W. Huang, "A review of early fault diagnosis approaches and their applications in rotating machinery," *Entropy*, vol. 21, no. 4, p. 409, 2019.

[7] D. Champier, "Thermoelectric generators: A review of applications," *Energy Conversion and Management*, vol. 140, pp. 167–181, 2017.